chemistry

MDPI

Review

New Materials and Phenomena in Membrane Distillation

Francesca Alessandro [1,*], Francesca Macedonio [1] and Enrico Drioli [1,2,*]

[1] Institute on Membrane Technology, National Research Council of Italy (CNR-ITM), Via P. Bucci 17/C, 87036 Rende, Italy
[2] Membrane Science and Technology Research Center, College of Chemical Engineering, Nanjing Tech University, Nanjing 211816, China
* Correspondence: f.alessandro@itm.cnr.it (F.A.); e.drioli@itm.cnr.it (E.D.)

Abstract: In recent decades, membrane-based processes have been extensively applied to a wide range of industrial processes, including gas separation, food industry, drug purification, and wastewater treatment. Membrane distillation is a thermally driven separation process, in which only vapour molecules transfer through a microporous hydrophobic membrane. At the operational level, the performance of membrane distillation is negatively affected by wetting and temperature polarization phenomena. In order to overcome these issues, advanced membranes have been developed in recent years. This review, which focuses specifically on membrane distillation presents the basic concepts associated with the mass and heat transfer through hydrophobic membranes, membrane properties, and advances in membrane materials. Photothermal materials for solar-driven membrane distillation applications are also presented and discussed.

Keywords: membrane distillation; temperature polarization; heat and mass transport; membrane materials

Citation: Alessandro, F.; Macedonio, F.; Drioli, E. New Materials and Phenomena in Membrane Distillation. *Chemistry* **2023**, *5*, 65–84. https://doi.org/10.3390/chemistry5010006

Academic Editor: Bartolo Gabriele

Received: 1 December 2022
Revised: 20 December 2022
Accepted: 23 December 2022
Published: 2 January 2023

1. Introduction

Membrane processes meet the Process Intensification (PI) requirements because they can potentially replace traditional energy-intensive techniques and increase the efficiency of reactive processes [1]. The significant advantages of membrane operations regard their low direct energy consumption and the opportunity to reduce indirect energy consumption through the recycling and reuse of raw materials [1,2].

Membrane technology finds applications in many fields of science and industry, including seawater desalination [3–5], wastewater treatment [6,7], produced water [8–10], food processing [11–16], textile industry [17–19], pharmaceutical applications [20–24] and chemical industry [25,26]. The first generation of membrane technologies includes pressure-driven processes, such as reverse osmosis (RO), nanofiltration (NF), and ultrafiltration (UF). Optimized membranes are required for these applications to meet the requirements of each membrane separation process and the corresponding operating conditions.

Pressure-driven processes need membranes operating at high pressures (5–30 bars) in order to achieve high productivity. Consequently, they require hydrophilic robust membranes with high mechanical strength able, therefore, to withstand severe operating conditions.

Over the last few decades, membrane distillation (MD) has attracted much attention, leading to the emergence of second-generation membrane processes. MD is a separation process in which only vapour molecules pass across a hydrophobic membrane. To date, polymeric membranes are the most commonly used membranes in MD technology because of their inherent hydrophobic properties and good processability [27]. However, the main drawbacks of MD operating with conventional membranes are represented by the wetting and temperature polarization. The latter, in particular, reduces the net driving force to mass transport and, ultimately, decreases the overall efficiency of the process. For this

reason, MD is still a technologically not mature process. Therefore, the development of advanced membranes that maximize MD's efficiency is required to enable its industrial-scale implementation.

This review describes the heat and mass transfer processes involved in MD, the main membrane properties, the recent advances in membrane materials, and the advent of thermoplasmonics in MD.

2. Membrane Distillation

Membrane distillation is an emerging thermal separation method that uses a microporous hydrophobic membrane in contact with a heated aqueous solution on the one hand (feed or retentate) and a condensing phase (permeate or distillate) on the other [28]. In this process, the hydrophobic membrane does not act as a conventional barrier or filter but supports the exchange of mass and energy between two opposing surfaces according to the principles of phase equilibrium [28].

Some of the key benefits of MD include: (i) lower operating temperatures compared to those typically used in the conventional distillation columns, allowing the use of low-grade heat streams such as alternative energy sources (solar, wind, or geothermal), (ii) theoretically removes 100% of all non-volatiles and (iii) achieves higher water recovery rates with respect to RO and conventional thermal processes, reducing the amount of brine released into the environment.

However, MD presents some drawbacks such as (i) the absence of membranes and modules specifically developed for MD, (ii) the risk of membrane pore wetting, and (iii) the polarization temperature associated with heat transfer through the membrane.

Generally, MD has been used for desalination applications [29–31] as an alternative to RO processes or to improve the limited recovery factor of RO and other thermal desalination techniques [32]. In addition, MD systems have been deemed a viable technology in arid areas located in regions with plenty of sun further limiting its application mainly to desalination [33,34]. Nevertheless, MD has been used in many other applications due to its reduced fouling tendency and its potential to handle complex solutions. The basic temperature gradient nature of the process also opens up new usage opportunities for vapour/gas separation applications where the equilibrium composition at any temperature is enriched with the more volatile component [32]. As a result, the scope of the process has extended beyond the traditional use of desalination. In addition to the conventional membrane-based processes, MD has the potential for temperature-sensitive products such as pharmaceutical compounds, juices, dairy products, natural aromatic compounds, and solutions of several chemicals. The process can be applied in fields where a very high rejection of certain components is required such as the treatment of nuclear waste or radioactive water [35] and water for the semiconductor industry [36].

2.1. Membrane Distillation Configurations

Depending on the way the water vapour is condensed, MD can be classified into four basic configurations (Figure 1): direct contact membrane distillation (DCMD), air gap membrane distillation (AGMD), sweep gas membrane distillation (SGMD), and vacuum membrane distillation (VMD).

Because of its simplicity, DMCD has been extensively investigated, despite its low efficiency. In the DCMD configuration, both hot feed and cold solutions are in direct contact with the membrane surface [37]. Volatile components of the feed solution vapourise at the hot feed side of the membrane, diffuse through the membrane pores and finally condense into the cold permeate side of the membrane. The main drawback of DCMD configuration is due to heat loss by conduction, which increases the amount of energy required to keep the solution hot enough to drive evaporation [3].

AGMD represents the most versatile technique in which only the feed solution is directly in contact with the hot side of the membrane. A thin air gap separates the hydrophobic membrane from the cold condensing surface, providing the possibility of condensing

the permeate vapours on the cold surface rather than directly in a cold liquid [38]. This corresponds to a considerable reduction in the amount of heat lost by conduction through the membrane [39]. However, in AGMD systems, with respect to the DCMD or VMD configurations [39–41], the fluxes are reduced because the air gap creates additional resistance to mass transfer. AGMD can be used for both DCMD applications and for removing volatile components as traces of aqueous alcohol solutions.

Combining the advantages of AGMD and DCMD, the SGMD configuration provides low conductive heat loss and low mass transfer resistance [42]. To maintain the gradient necessary for transport, an inert gas sweeps the vapour on the permeate side of the membrane [43]. This process has the primary benefit of reducing the mass transport resistance of the air gap. However, because a small volume of permeate diffuses into a large sweep gas volume, large external condensers are necessary to condense the vapour water and collect the permeate [44]. SGMD is mostly used for the removal of volatile organic compounds or dissolved gases from aqueous solutions.

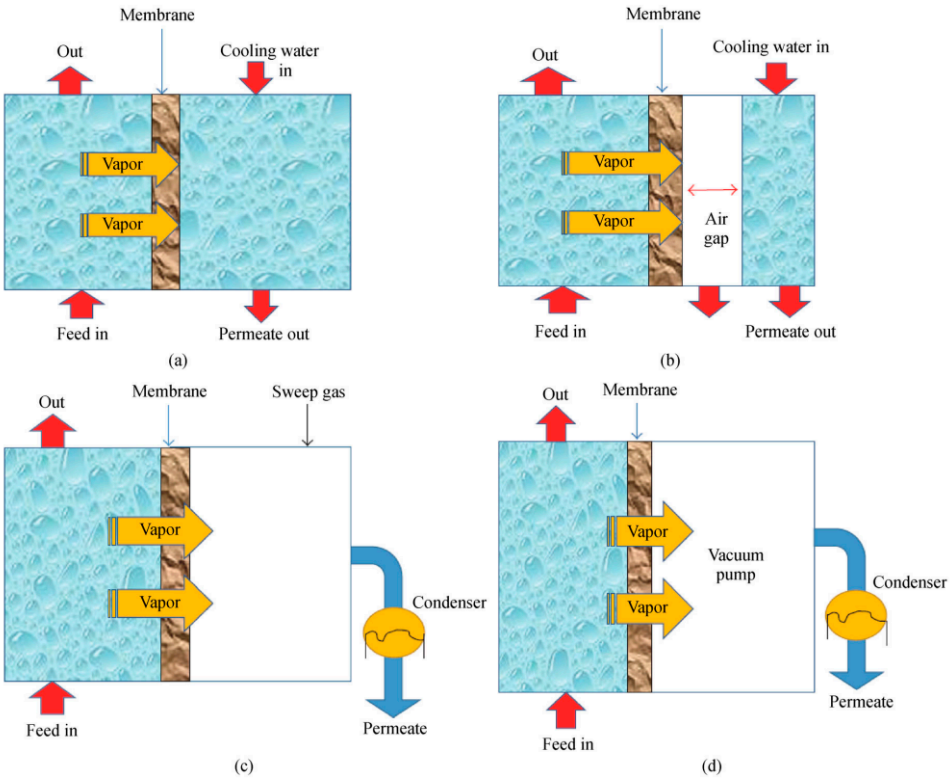

Figure 1. Membrane distillation basic configurations: (**a**) Direct contact membrane distillation (DCMD); (**b**) Air gap membrane distillation (AGMD); (**c**) Sweep gas membrane distillation (SGMD); (**d**) Vacuum membrane distillation (VMD). Reprinted from ref. [45] (Open access).

The VMD process is recognized as a cost-effective membrane separation method which can overcome many of the limitations of other MD systems. VMD applies a vacuum to the permeate side of the membrane, which allows it to operate at lower temperatures and pressures [45,46]. Consequently, thermal evaporation efficiency is increased, and the energy consumption is reduced.

Despite its high efficiency, MD technology is still limited on an industrial scale due to its low thermal efficiency. The specific energy consumption of traditional MD configurations can be easily above 1256 kWh m^{-3} (estimated from the gain output ratio, GOR) [47]. In recent years, new configurations have been proposed to reduce the specific energy consumption. Various MD configurations have been developed to harvest waste heat by internal heat recovery of the MD module. In particular, multi-stage and multi-effect membrane distillation (MEMD) systems have been designed to reduce energy consumption.

In the late 1990s, the Netherlands Organization for Applied Scientific Research (TNO) developed the AGMD Memstill MD with a heat recovery module, which was licensed to Aquastil and Keppel Seghers for commercialization. Memstill reported a very low specific energy consumption of 56–100 kWh m^{-3} [48]. Scarab Development AB (Sweden) developed a heat-recovery AGMD module with a plate-and-frame design [49]. An energy consumption of 810 kWh m^{-3} was achieved with a microporous PTFE membrane from GoreTex [50]. Vacuum multi-effect membrane distillation (V-MEMD) is a similar concept to MEMD, where efficiency is increased with the help of vacuum. V-MEMD consists of a heater, multiple evaporation–condensation stages, and an external condenser [51]. By recovering condensation heat from each stage, V-MEMD processes reduce specific energy consumption to 175–350 kWh m^{-3} [51].

2.2. Membrane Modules

Tubular module and plate and frame module represent the two main MD module configurations.

A hollow fiber (HF) tubular module consists of HF membranes enclosed into a housing as shown in Figure 2a. The feed is introduced into the shell side of the HFs, and cooling fluid, sweeping gas, or negative pressure can be applied on the other side to form VMD, SGMD, or DCMD [52]. Due to their large active area and small size, HF modules have a high potential for commercial applications. Good flow distribution on the shell side can be achieved using cross-flow modules that reduce the temperature polarization.

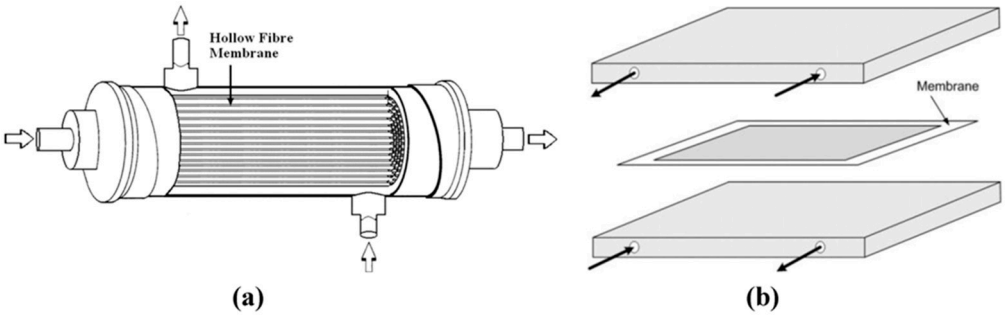

Figure 2. Membrane distillation modules: (**a**) Tubular module for hollow fiber; (**b**) Plate and frame module for flat sheet membrane. Open access. Reprinted from ref. [52] (Open access).

The plate and frame module (Figure 2b) is suitable for flat sheet membranes and can be used in DCMD, AGMD, VMD, and SGMD configurations [52]. This setup is easy to carry out and the effective area can be increased using multiple layers of flat sheet membranes. Flow dynamics can be improved by the use of spacers and baffles in order to increase turbulence and homogenize the temperature distribution inside the channels [36].

2.3. Mass and Heat Transfer

2.3.1. Mass Transfer

Water vapour flux is influenced by several factors, including feed and cold solution temperatures, and hot and cold stream velocities. A high operating temperature is generally preferred in MD processes. In MD system the water vapour flux J across the membrane is given by:

$$J = C \cdot \Delta P \quad (1)$$

where ΔP is the vapour pressure difference among the warm and cold sides of the membrane and C is a membrane distillation coefficient associated whit the membrane structure and flow parameters of the aqueous solution. This equation establishes a direct relationship between the water vapour flux and the driving force for mass transfer [38]. During this process, heat is also transferred, thus heat and mass transfer are closely linked with the consequent development of concentration and temperature profiles [38]. Mass transfer

is also induced by temperature differences across the membrane, which create a thermal gradient in the fluid phase, due to the Soret effect [53,54].

Figure 3a shows the possible mass transfer resistances in MD process with an electrical analogy. This approach considers the mass transfer in MD in terms of serial resistances upon the transfer between the bulks of two phases in contact with the membrane [28].

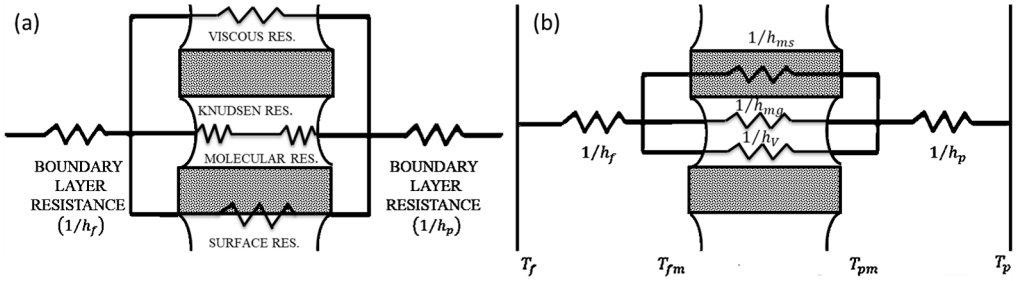

Figure 3. (**a**) Mass transfer and (**b**) heat transfer in membrane distillation.

The mass balance across the feed side boundary layer yields the relationship between molar flux N, the mass transfer coefficient k_x, the solution density ρ, and the solute concentrations c_m and c_b at the membrane surface and in the bulk, respectively [55]:

$$\frac{N}{\rho} = k_x ln \frac{c_m}{c_b} \tag{2}$$

The mass transfer coefficient is usually determined using empirical relations that can be expressed in the form

$$Sh = \alpha Re^{\beta} Sc^{\gamma} \tag{3}$$

where:

- Sh is the Sherwood number, $Sh = kd/D$ (d: hydraulic number, D: diffusion coefficient)
- Re is the Reynolds number, $Re = (\rho v d)/\mu$ (ρ: fluid density; ν: fluid velocity, μ: fluid viscosity)
- Sc is the Schmidt number, $Sc = \mu/\rho D$

more details are available in Refs. [56,57].

Due to the solvent flux through the membrane, the concentration of the non-volatile solutes at the membrane surface becomes higher than that at the bulk solution. To quantify the mass transport resistance within the boundary layer at the feed side, it is generally used the concentration polarization coefficient (CPC) given by the following equation:

$$CPC = \frac{C_m}{C_b} \tag{4}$$

Regarding the mass transport across the porous membrane, it is affected by:

- Knudsen diffusion resistance (due to collisions among the molecules and the membrane walls) [28]
- viscous resistance (due to the momentum transferred to the membrane) [28]
- molecular resistance (due to collisions between diffusing molecules) [28].

For mass transport through porous media, the dusty gas model (DGM) [58,59] is a useful general model

$$\frac{N_i^D}{D_{ie}^k} + \sum_{j=1 \neq i}^{n} \frac{p_j N_i^D - p_i N_j^D}{D_{ije}^0} = -\frac{1}{RT} \nabla p_i \tag{5}$$

$$N_i^v = -\frac{\varepsilon r^2 p_i}{8RT\tau\mu} \nabla P \tag{6}$$

$$D_{ie}^{k} = \frac{2\varepsilon r}{3\tau}\sqrt{\frac{8RT}{\pi M_i}} \tag{7}$$

$$D_{ije}^{0} = \frac{\varepsilon}{\tau} D_{ij}^{0} \tag{8}$$

where N^D is the diffusive flux, N^v is the viscous flux, D^k is the Knudsen diffusion coefficient, D^0 is the ordinary diffusion coefficient, p_i is the partial pressure of the component i, P is the total pressure, M_i is the molecular weight of component i, r is the membrane pore radius, ε is the membrane porosity, μ is the fluid viscosity, and τ is the membrane tortuosity. Underscript e indicates the "effective" diffusion coefficient.

The Knudsen-molecular diffusion transition for DCMD can be expressed as [58]:

$$N_i = \frac{-1}{RT}\left[\frac{1}{D_{1e}^{k}} + \frac{p_{air}}{D_{ije}^{0}}\right]^{-1} \nabla p_i \tag{9}$$

The DGM applied to VMD configuration, gives [60]:

$$N_i = \frac{2\varepsilon r}{3\tau RT}\left(\frac{8\ RT}{\pi M_i}\right)^{1/2} \Delta p_i. \tag{10}$$

2.3.2. Heat Transfer

The heat transfer in MD process (Figure 3b) can be summarized in three steps:

(1) convection from the feed bulk to the vapour–liquid interface at the membrane surface [61]

$$Q_f = h_f \cdot \left(T_f - T_{fm}\right) \tag{11}$$

(2) evaporation and conduction through the microporous membrane

$$Q_v = h_v \cdot \left(T_{fm} - T_{pm}\right) = N\Delta H_v \tag{12}$$

$$Q_c = \frac{k_g \cdot \varepsilon + k_m(1-\varepsilon)}{\delta_m} \cdot \left(T_{fm} - T_{pm}\right) \tag{13}$$

(3) convection from the vapour–liquid interface at the membrane surface to the permeate side [61]

$$Q_p = h_p \cdot \left(T_{pm} - T_p\right) \tag{14}$$

where Q_v is the heat transferred across the membrane due to the liquid evaporation at the surface of the membrane, Q_c is the heat transferred across the membrane material and via the vapour which fills the pores, N is the rate of mass transfer, ΔH_v is the latent heat of vapourisation, k_g is thermal conductivity of the vapour within the membrane, k_m is the thermal conductivity of the solid membrane material, ε is the membrane porosity, δ_m is the membrane thickness, T_{fm} is the temperature of the feed at the membrane surface, T_{pm} is the temperature of the permeate at the membrane surface, and T_f and T_p are the temperatures of the feed and permeate in the bulk, respectively.

The total heat (Q_T) transferred across the membrane is expressed by the following equation [60]:

$$Q_T = Q_v + Q_c = U\Delta T_b \tag{15}$$

where ΔT_b is bulk temperature difference among the feed and permeate sides and U is the overall heat transfer coefficient given by:

$$U = \frac{1}{h_f} + \frac{1}{\left(\frac{k_g \cdot \varepsilon + k_m(1-\varepsilon)}{\delta_m}\right) + \left(\frac{N\Delta H_v}{T_{fm} - T_{pm}}\right)} + \frac{1}{h_p} \quad (16)$$

Based on Equation (16), it is important to minimize boundary layer resistances maximizing boundary layer heat transfer coefficients. In order to quantify the extent of boundary layer resistance over total heat transfer resistance, a temperature polarization coefficient (TPC) is used [60]:

$$TPC = \frac{T_{fm} - T_{pm}}{T_f - T_p} \quad (17)$$

The boundary layer heat transfer coefficients are commonly evaluated using empirical correlations expressed as follows:

$$Nu = \alpha Re^{\beta} Pr^{\gamma} \quad (18)$$

where Nu is the Nusselt number, Re is the Reynolds number, Pr is the Prandtl number, and α, β, γ are the correlation coefficients dependent upon specific hydrodynamic conditions.

3. Membrane Properties

Obtaining high performance for MD process requires membranes with a specific structure and chemistry. The properties of membranes suitable for MD should include:

(i) An adequate thickness, based on a compromise between increased membrane permeability and reduced thermal resistance as the membrane becomes thinner [52].
(ii) Reasonably large pore size and narrow pore size distribution, limited by the minimum Liquid Entry Pressure (LEP) of the membrane [52].

The Liquid Entry Pressure is defined as the minimum transmembrane pressure that a feed solution requires to penetrate the hydrophobic membrane. LEP is a very important parameter for MD membranes, where the desired property of the membrane is to avoid the wetting of the pores.

In MD, the hydrostatic pressure must be lower than LEP to avoid membrane wetting [52]. This can be quantified by the following Laplace (Cantor) [62,63]

$$LEP_W = -\frac{2B\gamma_l \cos\theta}{r_{max}} < P_{process} - P_{pore} \quad (19)$$

where B is a geometric factor determined by pore structure (for instance, $B = 1$ for cylindrical pore), γ_l is the liquid surface tension, θ is the liquid/solid contact angle between water and the membrane surface, r_{max} is the maximum pore size, $P_{process}$ is the liquid pressure on either side of the membrane, and P_{pore} is the air pressure in the membrane pore.

Wetting occurs when the hydrostatic pressure on the feed side of the membrane exceeds LEP. The contact angle θ that gives information on the hydrophobicity of a membrane: a drop of water deposited on a hydrophobic surface gives a contact angle greater than 90°. In its simplest form, the wettability (Figure 4a) of a liquid droplet on a flat smooth surface is commonly determined by Young's equation [64]:

$$\gamma_{LV} cos\theta = \gamma_{SV} - \gamma_{SL} \quad (20)$$

where γ_{LV}, γ_{SV}, and γ_{SL} are the surface tension of liquid–vapour, polymer, and of solid-liquid, respectively.

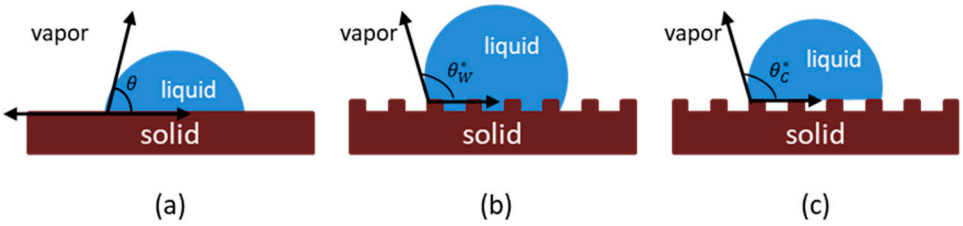

Figure 4. Schematic illustration of the Young (**a**), Wenzel (**b**), and Cassie–Baxter (**c**) models.

However, real membranes are not homogeneous and smooth. Therefore, the Young model is not applicable to them. The topography of roughness structure is taken into account by the Wenzel model [60] and the Cassie–Baxter model [61]:

$$\cos\theta_W = r\cos\theta \tag{21}$$

$$\cos\theta_C = f_s(\cos\theta + 1) - 1 \tag{22}$$

where r is the roughness factor in the Wenzel model, θ_C and f_s are, respectively, the apparent contact angle and the area fraction of the solid phase in the Cassie model, and θ is the ideal contact angle.

The Wenzel model considers a homogeneous wetting process where liquid fills in the grooves of a rough surface, increasing the liquid–solid interface surface area geometrically, as shown in Figure 4b. Instead, in Cassie–Baxter's model, droplets sit partially on air trapped in asperity valleys, indicating a heterogeneous wetting state (Figure 4c).

(iii) Low surface free energy. Surface-free energy can provide useful information about wetting potential of the feed solution with surface tension.
(iv) Low thermal conductivity. High thermal conductivities reduce vapour flux increasing heat transfer.
(v) High porosity. Membrane porosity is the volume fraction of the pores of the membrane. Membranes with greater porosity have a larger surface area for evaporation. So, a membrane with high porosity has higher permeate flux and lower conductive heat loss. Nevertheless, high-porosity membranes tend to break because of their low mechanical resistance. This results in a loss of membrane performance [52].

Membrane porosity (ε) can be determined by gravimetric method, measuring the weight of liquid contained in the membrane pores [65]

$$\varepsilon = \frac{(W_1 - W_2)/\rho_k}{(W_1 - W_2)/\rho_k + W_2/\rho_P} \cdot 100\% \tag{23}$$

where W_1 is the weight of the wet membrane, W_2 the weight of the dry membrane, ρ_k the density of the liquid, and ρ_P the polymer density.

In general, membranes used in MD systems have a porosity as high as 70–80%.

4. Advances on MD Membrane Materials

4.1. Polymeric Membranes

As previously mentioned, MD technology requires the use of hydrophobic membranes. Over the past few decades, among hydrophobic materials, fluoropolymers have attracted significant attention due to their high thermal stability, low surface tension, and good chemical resistance [66,67].

An important fluoropolymer used for fabricating MD membranes is Poly(Vinylidene Fluoride) (PVDF). PVDF is a semicrystalline polymer with typical crystallinity between 35% and 70% [68]. The crystalline phase of PVDF has five distinct crystal polymorphs: α (phase II), β (phase I), γ (phase III), δ, and ε. The α-form is the most common non-polar phase formed of $(CH_2–CF_2)$n chains in a monoclinic crystallographic form whereas the

polar β-phase is the most thermodynamically stable form. This latter is of special interest due to its pyro- and piezoelectric properties.

PVDF shows a good thermal stability, mechanical, and chemical resistance, and it can be dissolved in mostly common solvents such as N-methyl-2-pyrrolidone (NMP), N,N–dimethyl acetamide (DMAc), and N,N–dimethyl formamide (DMF) [68]. It has a glass transition temperature (Tg) in the range from −40 °C to −30 °C and a melting point between 155 °C and 192 °C.

As regards the synthesis processes, nonsolvent-induced phase separation (NIPS) technique is mainly used for the production of PVDF membranes for MD applications. In the membrane-preparation process via NIPS, polymer solution is immersed in a nonsolvent bath, inducing phase separation of solution into a polymer-rich (membrane matrix) phase and a polymer-poor phase (membrane pores) [69].

Other techniques used to synthesize PVDF membranes are thermally induced phase separation (TIPS) and electrospinning. In the TIPS process, the membrane formation is induced by cooling the polymer solution. Some of the advantages of TIPS are the simplicity of the method, high porosity, and the capability to form narrow pore size distribution [70]. Recently, the electrospinning process has also attracted considerable attention mainly due to the fact that it is a simple process to produce submicron and nano-scale fibers. In comparison to the membrane produced by NIPS, the electrospun membranes exhibit superior porosity, a high-specific surface area, and a high strength-to-weight ratio [68,71].

To reduce fouling or increase wetting resistance, various modifications have been suggested such as surface coating, blending and pore filling [72].

The mechanical stability of PVDF membranes can be enhanced by using PVDF-Hyflon AD super-hydrophobic membranes [73]. The fluorinated polymer Hyflon AD, with its excellent mechanical and hydrophobic properties, is ideal for producing PVDF-Hyflon composite membranes. Wet chemical treatment and dry-wet phase inversion can be used to design these membranes.

PVDF mixed matrix membranes incorporating Cloisite15A were tested in DCMD for the treatment of rubber processing effluents [74]. MD tests showed a significant reduction in flux over time. However, high removal efficiencies have been achieved.

Mokhtar et al. [75] prepared PVDF HF membranes blended with ethylene glycol (EG) and investigated their performance in DCMD tests on the treatment of dye solution system. The membranes were prepared by dry-jet wet spinning method. The results showed that the modified PVDF membrane was able to produce consistent flux (9.71 kg m^{-2} h^{-1} after 6 h-experiment at 60 °C) throughout the experiment while maintaining excellent dye rejection (>99.75%).

Another polymer widely used for the MD membrane production is Polytetrafluoroethylene (PTFE), better known by the trade name Teflon. It is a thermoplastic polymer and it is formed by carbon chains having two fluorine atoms for each carbon atom. The most important properties of PTFE (such as high chemical stability, high heat resistance, and strong hydrophobicity) derive from the strong C-C and C-F bonds and the carbon backbone. The latter is protected against chemical attacks by a uniform and continuous coverage consisting of fluorine atoms. PTFE is electrically inertness, so volume and surface resistivity are high. It is insoluble in common solvents at room temperature. Additionally, PTFE is highly crystalline (92–98% crystallinity) and the crystallites have a high melting point (342 °C) which makes the processability of PTFE difficult. Therefore, the commonly used phase inversion or melt spinning techniques for membrane synthesis cannot be exploited for PTFE. Currently PTFE membranes are prepared using complicated extrusion, rolling, stretching and sintering methods which make difficult the control of the porous structure [76].

Properties such as low-cost, good thermal stability, chemical resistance and mechanical strength make the polypropylene (PP) suitable for membrane applications. PP consists of a repeating unit, $–CH_2CH(CH_3)$ monomer. It exists in both semi-crystalline and amorphous forms but the Isostatic PP, a semicrystalline form, is the most commonly used for

commercial-scale membrane preparation. Moreover, as compared to PVDF, PP has low hydrophobicity due to its high surface energy.

PP membrane is fabricated using the following three main techniques: TIPS, stretching, and track-etching. The stretching method is a solvent free technique and is applicable for the semicrystalline polymers. It consists of four fundamental processes: the molten polymer film is extruded into a film (1) which is subsequently annealed (2); annealing is followed by cold and hot stretching (3) that generated and enlarges the pore size; to avoid pore closure, heat setting is performed as the last step (4). The track-etching technique is mainly based on the use of heavy-ion accelerators.

With this technique, the pore size and density can be controlled to produce membranes having the required transport properties.

Future research is expected to be directed towards investigating novel preparation methods for PP membranes using, in particular, less-explored techniques such as electrospinning. Furthermore, the use of fillers such as carbon nanotubes (CNTs) can also be investigated to create membranes having specific properties [77].

New fluoropolymers have recently received attention for improving MD membrane performance.

One example of this is poly(ethylenechlorotrifluoroethylene) (ECTFE) [66,78], often referred to as HALAR by Solvay Specialty Chemicals, a very appealing candidate for MD applications due to its high hydrophobicity. It is mechanically stable under a wide range of temperatures. In addition, it has excellent solvent and chemical resistance properties that make it suitable for applications under harsh conditions. The major disadvantage of ECTFE-based membranes is the need to fabricate the membranes at extremely high temperatures.

Hyflon AD from Solvay Specialty Polymers and Cytop from Asahi Glass are also interesting polymers examples for MD systems [66,79,80]. These polymers are highly soluble in fluorinated solvents and have a low solution viscosity, making them potential membrane synthesis candidates. Hyflon-coated PVDF membranes also show high hydrophobicity, narrow pore sizes, and high mechanical strength [80].

4.2. Ceramic Membranes

PVDF, PTFE, and PP membranes demonstrate some drawbacks in terms of thermal and chemical stabilities that can limit their lifetime [81]. As a result, hydrophobic ceramic membranes have attracted considerable interest because of their exceptional characteristics that allow long-term operation without significant performance degradation.

Alumina, iron, silica, titania, and zirconia metal oxides are widely used to produce ceramic membranes. Depending on the pore size of the bulk material, the ceramic membranes can be intrinsically selective or may consist of a thin layer supported by a porous alumina substrate [52]. Ceramic membranes usually exhibit a more homogeneous morphology than polymeric membranes. Although the majority of the work uses commercial support materials, additional research has explored the use of natural clay to treat thin membranes, such as aluminum phyllosilicates. Compared with the competing organic membranes, ceramic membranes perform better in harsh environments, e.g., at temperatures above 200 °C or during solvent separation, due to the superior thermal, chemical, and mechanical stabilities of ceramics. Furthermore, unlike polymeric membranes, ceramic membranes are resistant to chemically aggressive feeds. In fact, ceramic membranes can be used with a wide variety of organic solvents, without significant degradation [52].

For specific purification fields, such as filtering, extraction, desalination, crystallization, and gas separation, functionalized ceramic membranes have become more attractive than intrinsically hydrophilic ceramic membranes.

The surface characteristics of membranes directly influence their properties, such as hydrophobicity, oleophobicity, adhesion, scaling behaviour, and surface charges. Due to their abundance of hydroxyl groups (-OH), ceramic membranes exhibit hydrophilic behaviour [82,83], making them unsuitable for MD. As a result, many strategies have been

investigated for changing the membrane surface from hydrophilic to hydrophobic, including fluorination, electrospun nanofibers, growth of silica gels, and nanostructuring [84].

Few studies have been conducted on ceramic membranes for MD. The first work was realized in 2004 [85], in which the possibility of applying ceramic membranes to MD was demonstrated by grafting the metal oxides Al_2O_3 and ZrO_2 with fluoroalkylsilanes, which were subsequently applied to DCMD.

To improve membrane ceramic performance, hydrophobic Al_2O_3 ceramic HFs for VMD were developed [86]. Furthermore, the use of ceramic membranes in MCr was demonstrated for the first time in 2018 [87].

4.3. Omniphobic Ceramic Membranes

Conventional hydrophobic membranes are susceptible to wetting by low- surface-tension contaminants in the feed solution. The wetted membrane pores result in higher mass transfer resistance to water vapour diffusion during MD. To overcome this problem, omniphobic surfaces with re-entrant structures that are resistant to being wetted by low-surface tension liquids can be fabricated.

Ceramic membranes have recently been prepared as substrates [88,89]. By depositing nanostructures on ceramic membrane surfaces, surface roughness was increased, and a re-entrant structure was created.

Chen et al. [90] prepared omniphobic alumina HF membranes by depositing ZnO nanostructures on HF membranes through chemical bath deposition methods. In the DCMD tests, the HF membranes deposited by ZnO nanoparticles showed greater wetting resistance compared to the pristine HF membrane. This result suggests the promising use of these membranes for the desalination of low-surface-tension wastewater.

4.4. New Materials

4.4.1. Graphene

Graphene-based nanomaterials such as graphene oxide (GO) and reduced graphene oxide (rGO) offer new possibilities for MD membrane production. Due to their unique features such as high hydrophobicity, high mechanical resistance, large surface area, and high chemical stability, the use of graphene and its derivates in MD membranes allows for achieving greater flow and strength, lower energy consumption, and enhanced antifouling capabilities. In mixed matrix membrane fabrication, graphene-based nanomaterials can be effectively used as a filler [91]. Recently, mixed matrix graphene oxide polysulphone (GO-PSF) membranes were prepared with variable GO content using the wet phase inversion method [92]. In DCMD experiments, the membrane containing 1.0 wt.% GO offered the highest salt rejection (99.85%) with an average flux of 20.8 L m^{-2} h^{-1} [92] and a permeate conductivity of 85.20 mS/cm [92]. In comparison with the pristine PSF membrane, the GO/PSF membrane exhibits higher mechanical properties.

PVDF/GO and PVDF/3-(aminopropyl)triethoxysilane (APTS)-functionalized GO mixed matrix membranes were prepared via the inversion phase method and used to desalinate artificial seawater with AGMD [93]. As a result of adding GO and GO-APTS, the permeate flux increased by 52% and 86%, respectively, compared to pure PVDF. The best-performing membrane contained 0.3 wt.% GO-APTS (with respect to PVDF) and had a flux of 6.2 LMH (L m^{-2} h^{-1}) whilst maintaining perfect salt rejection (>99.9%) [93].

Reducing the membrane thickness is one of the key methods for increasing membrane flux. Composite membranes provide this condition. A composite membrane usually consists of a porous support and a permselective thin layer deposited on it. In MD applications, the composite membrane should have at least one hydrophobic layer. Grafting (functionalization), coating, surface polymerization, and co-extrusion dry/wet jet spinning [52,94] are some of the most common methods of fabricating composite membranes.

A PVDF-HFP/GO hollow fiber membrane was fabricated using the dry/wet jet spinning method and functionalized with hydrophobic octadecyltrichlorosilane (ODS) for desalination using DCMD [95]. The incorporation of GO in the membrane matrix induces

the hierarchy roughness on the membrane surface and provides reactive hydroxyl sites for further chemical modification. Desalination of Caspian Sea water (CSW) was conducted using prepared membranes through DCMD. Modified membranes showed partial salt precipitation and permeation flux reduction after 10 days [95].

The main disadvantage of graphene is its high thermal conductivity which limits its use in MD applications. Gontarek et al. [96] investigated the effects of confinement of multilayer graphene platelets in hydrophobic microporous polymeric membranes. Despite the filler exhibits ultrahigh thermal conductivity, no thermal polarization was observed. In contrast, improved wetting resistance and mechanical strength, represent the essential requirements for MD applications.

The improvement of the flux-selectivity trade-off is considered one of the main challenges for membrane processes. Frappa et al. [97] proposed advanced PVDF membranes incorporating few-layer graphene for water treatment by MD. The membranes were prepared by the innovative wet-jet milling technique [98]. An increase of 99.7% in flux have been observed for the PVDF membrane filled with few-layer graphene compared to the virgin PVDF membrane [97]. Additionally, a comparison between membranes based on PVDF enhanced with different fillers shows a significant enhancement of the productivity–efficiency trade-off for PVDF membrane graphene-based produced via wet-jet milling (Figure 5).

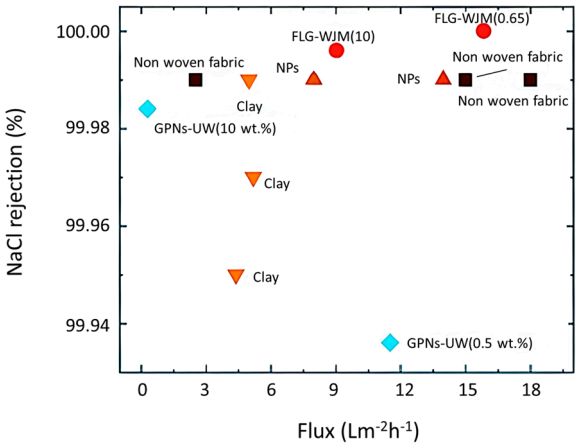

Figure 5. Productivity–efficiency trade–off diagram for PVDF membranes based on different fillers: graphene obtained by wet-jet milling process (red circles), graphene produced by ultrasonic waves (blue diamonds) [99], clay (orange triangles) [100], nonwoven fabric (dark brown squares) [101], and nanoparticles (NPs) (brown triangles) [102]. (T_{FEED}: ~55 °C, except for the nanoparticles T_{FEED}: = 70 °C). Reprinted from ref. [97] (Open access).

4.4.2. Two-Dimensional Materials beyond Graphene

The exotic properties and atomic thickness of two-dimensional (2D) materials allowed for the development of a new generation of membrane materials with extraordinarily high permeabilities. MXenes [103], zeolites [31,104], and metal–organic framework [105] nanosheets have emerged as promising 2D materials for high-performance membranes. Two dimensional-material membranes, due to their well-defined transport channels and ultra-low thickness offer an ultra-low resistance to mass transport. Specifically, 2D membranes have been shown to perform exceptionally well in liquid and gas separation applications.

Recently, a dichalcogenide material (Bi_2Te_3) has been proposed for desalination of water by MD, for the first time [106]. The authors demonstrated that the use of Bi_2Te_3 (exfoliated and included in PVDF membranes) increases the freshwater production, contrasting the loose of conductive heat.

Scale-up of the 2D materials-based membranes is compromised by the limited available exfoliation techniques. In recent times, an important patent has been deposited related

the production of a nanocomposite membrane with 2D crystals obtained through the exfoliation of layered materials by wet-jet milling technique [98].

4.5. Carbon Nanotubes

Due to their exceptional mechanical strength, chemical resistance, and thermal properties, carbon nanotubes (CNTs) have gained significant attention. The structure of CNTs consists of an enrolled cylindrical graphitic sheet. The main features which make CNT an emerging nanomaterial in water desalination are their large specific surface area, high aspect ratio, ease of functionalization, high transport of water molecules, and the possibility to change the water–membrane interaction favouring the preferential transport of vapours through the pores [89,107–109]. Furthermore, CNT-based membranes exhibit outstanding porosity and hydrophobicity, basic requisites for MD applications. CNTs used as fillers have proven to significantly improve membrane performance in terms of strength, rejection, and permeability. In 2010, the first evidence was provided regarding the potential of CNT membranes for desalination by MD [110]. A significant increase in flow enhancement is observed when CNTs-based membranes are used in MD applications.

The main disadvantages are related to the long-term operation, synthesis, processing of CNTs, and scale-up approaches [111].

4.6. Hydrophilic/Hydrophobic Membranes

Hydrophilic-hydrophobic membranes can be used to enhance the flux in MD processes. These composite membranes were patented in 1982 by Cheng and Wiersma as an alternative approach for desalination applications. They modified a cellulose acetate membrane via radiation graft polymerization of styrene onto the membrane surface [112]. They also modified a cellulose nitrate membrane via plasma polymerization of both vinyltrimethylsilicon/carbon tetrafluoride and octafluoro-cyclobutane [94].

Zuo et al. [113] developed a dual-layer hydrophilic-hydrophobic HF using polyetherimide as the inner layer due to its good mechanical properties. As a result, the membrane exhibited good mechanical strength and higher water flux in VMD.

Recently, crosslinked PVDF-based hydrophilic-hydrophobic dual-layer HF membranes were fabricated for DCMD [114]. The water flux reached a value of 97.6 kg m^{-2} h^{-1} for seawater desalination and the membrane showed stable DCMD performance [114].

5. Photothermal Membrane for Membrane Distillation

In order to provide high-quality freshwater, solar energy combined with MD can be deemed a valid low-cost option [115–119]. Research on light-to-heat conversion in nanomaterials has opened up unprecedented prospects for solar energy-based MD applications. Recently, it has been demonstrated that the integration of photothermal nanofillers within membranes allows a significant reduction of thermal polarization, improving the energy efficiency of the process. Specifically, it has been proved that thermoplasmonics (the light-to-heat conversion associated with optically plasmonic excitations in metal nanoparticles) facilitates water vapourisation at photothermal interfaces [120–122]. Many classes of nanomaterials have emerged as potential candidates for converting light into heat [115]. In particular, photothermal materials can be divided into four main groups: metal nanostructures, semiconductors, carbon-based nanomaterials, and polymers.

Silver [123–125] and gold [126–128] are the most common photothermal materials due to their tunable absorption properties and chemical stability. In a pioneering study on photothermal VMD, Politano et al. [129] reported that Ag nanoparticles (NPs), immobilized in PVDF membranes by NIPS, notably increase the feed temperature at the membrane surface under UV light, so as to reduce temperature polaritation. An enhancement until 11-fold of the transmembrane flux was observed at the highest NP concentration. [129].

Other metallic (Cu [130], Al [131], Fe [131]) and bimetallic NPs (Fe–Au [132], Ag–Au [133] and Pd–Au [134]) also exhibited interesting thermoplasmonic properties.

Inorganic semiconductors, such as black TiOx [135], TiN [136], Cu_2–yX (X = S, Se, Te) [137], and MoS_2 [138], have emerged as promising thermoplasmonic materials due to their capability to tune plasmon surface responses via chemical doping and their flexibility to post-synthetically tune the plasmon surface characteristics. For instance, TiN photothermal membranes were prepared using a TiN NP/PVA-doped solution, spray-coated onto a hydrophobic PVDF membrane surface [136]. As a result of the absorption of broadband light and the superior heat conversion properties of plasmonic TiN NPs, the TiN photothermal membrane showed a permeate flux of 1.01 L m^{-2} h^{-1}, with a solar efficiency of 66.7% under 1 sun in the photothermal DCMD process.

Graphene, GO, rGO, CNT, carbon black (CB), and carbonized natural products [139–143] are also potential photothermal materials. In the same way as a black body, carbon-based materials absorb light and convert it into heat. The advantages of these materials include their low cost, their physico-chemical properties, and their environmental stability.

Evaporation method was employed to deposit CB NPs on a PVDF membrane and its performance was compared with SiO_2/Au anchored to the PVDF surface using polydopamine as a binder [142]. In photothermal DCMD, CB-PVDF membranes showed a flux of 0.5 kg m^{-2} h^{-1}, a much higher value compared to SiO_2/Au-PVDF membranes.

The possible use of polymers as photothermal materials was investigated for conjugated polymers including polyaniline (PANi) and polypyrrole (PPy) [144,145].

Recently, Peng et al. [146] reported a bio-inspired design of a photothermal membrane for solar-drivenMD, which is composed of a vertically-aligned PANi nanofiber layer on the surface of a PVDF microfiltration membrane. The photothermal membrane exhibited a distillation flux of 1.09 kg m^{-2} h^{-1} and a corresponding solar energy-to-collected water efficiency as high as 74.15% under one sun irradiation [146].

6. Conclusions and Outlook

Membrane distillation can provide new opportunities to design and optimize innovative productions. Some of the most exciting developments concern the ability to integrate new membrane devices with traditional membrane systems, with significant advantages connected to a synergic integration between them.

Notwithstanding its high potential, the industrial-scale MD operativity has been to date hindered by severe limitations associated with low thermal efficiency mainly due to temperature polarization. In order to overcome the existing limits, it is necessary to carry out an increasingly systematic analysis of the possible advantages or disadvantages concerning the introduction of an innovative membrane system, an increasingly appropriate choice of materials and operating conditions, as well as easier modelling for a facilitated scale-up. Therefore, the preparation of new and specific membranes with high hydrophobicity and stability, with a narrow pore distribution and better morphological properties, represents a crucial aspect to improve MD performances.

This review described the membrane materials and the most favourable membrane characteristics for the MD processes. Because of their intrinsic hydrophobic characteristics, ease of fabrication, and low cost, polymeric membranes are the most widely used in MD applications. Recently, two-dimensional materials, CNTs, ceramic and photothermal membranes have attracted much attention due to their unique properties that make them potential candidates for MD applications. However, the development of advanced membranes for MD applications is still in the early stages. Many efforts are still required to make them fully suitable for MD processes.

Author Contributions: Conceptualization, E.D. and F.M.; writing—original draft preparation, F.A.; writing—review and editing, E.D., F.M. and F.A.; supervision E.D. and F.M. All authors have read and agreed to the published version of the manuscript.

Funding: This research received no external funding.

Data Availability Statement: Not applicable.

Conflicts of Interest: The authors declare no conflict of interest.

References

1. Drioli, E.; Curcio, E. Membrane engineering for process intensification: A perspective. *J. Chem. Technol. Biotechnol.* **2007**, *82*, 223–227. [CrossRef]
2. Drioli, E.; Romano, M. Progress and new perspectives on integrated membrane operations for sustainable industrial growth. *Ind. Eng. Chem. Res.* **2001**, *40*, 1277–1300. [CrossRef]
3. Lado, J.J.; Cartolano, V.; García-Quismondo, E.; García, G.; Almonacid, I.; Senatore, V.; Naddeo, V.; Palma, J.; Anderson, M.A. Performance analysis of a capacitive deionization stack for brackish water desalination. *Desalination* **2021**, *501*, 114912. [CrossRef]
4. Chang, Y.S.; Ooi, B.S.; Ahmad, A.L.; Leo, C.P.; Low, S.C. Vacuum membrane distillation for desalination: Scaling phenomena of brackish water at elevated temperature. *Sep. Purif. Technol.* **2021**, *254*, 117572. [CrossRef]
5. Tufa, R.A.; Noviello, Y.; Di Profio, G.; Macedonio, F.; Ali, A.; Drioli, E.; Fontananova, E.; Bouzek, K.; Curcio, E. Integrated membrane distillation-reverse electrodialysis system for energy-efficient seawater desalination. *Appl. Energy* **2019**, *253*, 113551. [CrossRef]
6. Arola, K.; Van der Bruggen, B.; Mänttäri, M.; Kallioinen, M. Treatment options for nanofiltration and reverse osmosis concentrates from municipal wastewater treatment: A review. *Crit. Rev. Environ. Sci. Technol.* **2019**, *49*, 2049–2116. [CrossRef]
7. Obotey Ezugbe, E.; Rathilal, S. Membrane technologies in wastewater treatment: A review. *Membranes* **2020**, *10*, 89. [CrossRef]
8. Maltos, R.A.; Regnery, J.; Almaraz, N.; Fox, S.; Schutter, M.; Cath, T.J.; Veres, M.; Coday, B.D.; Cath, T.Y. Produced water impact on membrane integrity during extended pilot testing of forward osmosis–reverse osmosis treatment. *Desalination* **2018**, *440*, 99–110. [CrossRef]
9. Zou, L.; Gusnawan, P.; Zhang, G.; Yu, J. Novel Janus composite hollow fiber membrane-based direct contact membrane distillation (DCMD) process for produced water desalination. *J. Membr. Sci.* **2020**, *597*, 117756. [CrossRef]
10. Ali, A.; Quist-Jensen, C.A.; Drioli, E.; Macedonio, F. Evaluation of integrated microfiltration and membrane distillation/crystallization processes for produced water treatment. *Desalination* **2018**, *434*, 161–168. [CrossRef]
11. Chen, G.Q.; Gras, S.L.; Kentish, S.E. The application of forward osmosis to dairy processing. *Sep. Purif. Technol.* **2020**, *246*, 116900. [CrossRef]
12. Hausmann, A.; Sanciolo, P.; Vasiljevic, T.; Ponnampalam, E.; Quispe-Chavez, N.; Weeks, M.; Duke, M. Direct contact membrane distillation of dairy process streams. *Membranes* **2011**, *1*, 48–58. [CrossRef]
13. Cassano, A.; Conidi, C.; Drioli, E. A comprehensive review of membrane distillation and osmotic distillation in agro-food applications. *J. Membr. Sci. Res.* **2020**, *6*, 304–318.
14. Destani, F.; Naccarato, A.; Tagarelli, A.; Cassano, A. Recovery of aromatics from orange juice evaporator condensate streams by reverse osmosis. *Membranes* **2020**, *10*, 92. [CrossRef] [PubMed]
15. Kujawa, J.; Guillen-Burrieza, E.; Arafat, H.A.; Kurzawa, M.; Wolan, A.; Kujawski, W. Raw juice concentration by osmotic membrane distillation process with hydrophobic polymeric membranes. *Food Bioprocess Technol.* **2015**, *8*, 2146–2158. [CrossRef]
16. Julian, H.; Yaohanny, F.; Devina, A.; Purwadi, R.; Wenten, I.G. Apple juice concentration using submerged direct contact membrane distillation (SDCMD). *J. Food Eng.* **2020**, *272*, 109807. [CrossRef]
17. Fortunato, L.; Elcik, H.; Blankert, B.; Ghaffour, N.; Vrouwenvelder, J. Textile dye wastewater treatment by direct contact membrane distillation: Membrane performance and detailed fouling analysis. *J. Membr. Sci.* **2021**, *636*, 119552. [CrossRef]
18. Leaper, S.; Abdel-Karim, A.; Gad-Allah, T.A.; Gorgojo, P. Air-gap membrane distillation as a one-step process for textile wastewater treatment. *Chem. Eng. J.* **2019**, *360*, 1330–1340. [CrossRef]
19. Li, M.; Wang, X.; Porter, C.J.; Cheng, W.; Zhang, X.; Wang, L.; Elimelech, M. Concentration and recovery of dyes from textile wastewater using a self-standing, support-free forward osmosis membrane. *Environ. Sci. Technol.* **2019**, *53*, 3078–3086. [CrossRef]
20. Ray, H.; Perreault, F.; Boyer, T.H. Urea recovery from fresh human urine by forward osmosis and membrane distillation (FO–MD). *Environ. Sci. Water Res. Technol.* **2020**, *5*, 1993–2003. [CrossRef]
21. Yan, Z.; Yang, H.; Qu, F.; Zhang, H.; Rong, H.; Yu, H.; Liang, H.; Ding, A.; Li, G.; Van der Bruggen, B. Application of membrane distillation to anaerobic digestion effluent treatment: Identifying culprits of membrane fouling and scaling. *Sci. Total Environ.* **2019**, *688*, 880–889. [CrossRef]
22. Yadav, A.; Yadav, P.; Labhasetwar, P.K.; Shahi, V.K. CNT functionalized ZIF-8 impregnated poly (vinylidene fluoride-co-hexafluoropropylene) mixed matrix membranes for antibiotics removal from pharmaceutical industry wastewater by vacuum membrane distillation. *J. Environ. Chem. Eng.* **2021**, *9*, 106560. [CrossRef]
23. Woldemariam, D.; Kullab, A.; Fortkamp, U.; Magner, J.; Royen, H.; Martin, A. Membrane distillation pilot plant trials with pharmaceutical residues and energy demand analysis. *Chem. Eng. J.* **2016**, *306*, 471–483. [CrossRef]
24. El-Bourawi, M.S.; Ding, Z.; Ma, R.; Khayet, M. A framework for better understanding membrane distillation separation process. *J. Membr. Sci.* **2006**, *285*, 4–29. [CrossRef]
25. Pagliero, M.; Bottino, A.; Comite, A.; Costa, C. Novel hydrophobic PVDF membranes prepared by nonsolvent induced phase separation for membrane distillation. *J. Membr. Sci.* **2020**, *596*, 117575. [CrossRef]
26. Liu, C.; Dong, G.; Tsuru, T.; Matsuyama, H. Organic solvent reverse osmosis membranes for organic liquid mixture separation: A review. *J. Membr. Sci.* **2021**, *620*, 118882. [CrossRef]

27. Boo, C.; Lee, J.; Elimelech, M. Omniphobic polyvinylidene fluoride (PVDF) membrane for desalination of shale gas produced water by membrane distillation. *Environ. Sci. Technol.* **2016**, *50*, 12275–12282. [CrossRef]
28. Drioli, E.; Giorno, L. (Eds.) *Comprehensive Membrane Science and Engineering*; Newnes: Boston, MA, USA, 2010; Volume 1.
29. Sun, A.C.; Kosar, W.; Zhang, Y.; Feng, X. Vacuum membrane distillation for desalination of water using hollow fiber membranes. *J. Membr. Sci.* **2014**, *455*, 131–142. [CrossRef]
30. Donato, L.; Garofalo, A.; Drioli, E.; Alharbi, O.; Aljlil, S.A.; Criscuoli, A.; Algieri, C. Improved performance of vacuum membrane distillation in desalination with zeolite membranes. *Sep. Purif. Technol.* **2020**, *237*, 116376. [CrossRef]
31. Gopi, G.; Arthanareeswaran, G.; Ismail, A.F. Perspective of renewable desalination by using membrane distillation. *Chem. Eng. Res. Des.* **2019**, *144*, 520–537.
32. Ali, A. Evaluation of Membrane Characteristics and Thermal Polarization in Membrane Distillation. Ph.D. Thesis, Université Paul Sabatier-Toulouse III, Toulouse, France, 2015.
33. Chafidz, A.; Al-Zahrani, S.; Al-Otaibi, M.N.; Hoong, C.F.; Lai, T.F.; Prabu, M. Portable and integrated solar-driven desalination system using membrane distillation for arid remote areas in Saudi Arabia. *Desalination* **2014**, *345*, 36–49. [CrossRef]
34. Wang, W.; Shi, Y.; Zhang, C.; Hong, S.; Shi, L.; Chang, J.; Li, R.; Jin, Y.; Ong, C.; Zhuo, S.; et al. Simultaneous production of fresh water and electricity via multistage solar photovoltaic membrane distillation. *Nat. Commun.* **2019**, *10*, 3012. [CrossRef] [PubMed]
35. Khayet, M. Treatment of radioactive wastewater solutions by direct contact membrane distillation using surface modified membranes. *Desalination* **2013**, *321*, 60–66. [CrossRef]
36. Liu, C.; Martin, A.R. The use of membrane distillation in hugh-purity water production for the semiconductor industry. *Ultrapure Water* **2006**, *23*, 32–38.
37. Parani, S.; Oluwafemi, O.S. Membrane distillation: Recent configurations, membrane surface engineering, and applications. *Membranes* **2021**, *11*, 934. [CrossRef] [PubMed]
38. Gugliuzza, A.; Basile, A. Membrane contactors: Fundamentals, membrane materials and key operations. In *Handbook of Membrane Reactors*; Woodhead Publishing: Sawston, UK, 2013; pp. 54–106.
39. Noamani, S.; Niroomand, S.; Rastgar, M.; Azhdarzadeh, M.; Sadrzadeh, M. Modeling of Air-Gap Membrane Distillation and Comparative Study with Direct Contact Membrane Distillation. *Ind. Eng. Chem. Res.* **2020**, *59*, 21930–21947. [CrossRef]
40. Ansari, A.; Galogahi, F.M.; Thiel, D.V.; Helfer, F.; Millar, G.; Soukane, S.; Ghaffour, N. Downstream variations of air-gap membrane distillation and comparative study with direct contact membrane distillation: A modelling approach. *Desalination* **2022**, *526*, 115539. [CrossRef]
41. Yang, C.; Peng, X.; Zhao, Y.; Wang, X.; Cheng, L.; Wang, F.; Li, Y.; Li, P. Experimental study on VMD and its performance comparison with AGMD for treating copper-containing solution. *Chem. Eng. Sci.* **2019**, *207*, 876–891. [CrossRef]
42. Kalla, S.; Upadhyaya, S.; Singh, K. Principles and advancements of air gap membrane distillation. *Rev. Chem. Eng.* **2019**, *35*, 817–859. [CrossRef]
43. Xie, Z.; Duong, T.; Hoang, M.; Nguyen, C.; Bolto, B. Ammonia removal by sweep gas membrane distillation. *Water Res.* **2009**, *43*, 1693–1699. [CrossRef]
44. Alkhudhiri, A.; Hilal, N. Membrane distillation—Principles, applications, configurations, design, and implementation. In *Emerging Technologies for Sustainable Desalination Handbook*; Butterworth-Heinemann: Oxford, UK, 2018; pp. 55–106.
45. Alhathal Alanezi, A.; Abdallah, H.; El-Zanati, E.; Ahmad, A.; Sharif, A.O. Performance investigation of O-ring vacuum membrane distillation module for water desalination. *J. Chem.* **2016**, *2016*, 9378460. [CrossRef]
46. Criscuoli, A.; Bafaro, P.; Drioli, E. Vacuum membrane distillation for purifying waters containing arsenic. *Desalination* **2013**, *323*, 17–21. [CrossRef]
47. Kaleekkal, N.J.; Mural, P.K.S.; Vigneswaran, S.; Ghosh, U. (Eds.) . *Sustainable Technologies for Water and Wastewater Treatment*; CRC Press: Boca Raton, FL, USA, 2021.
48. Jansen, A.E.; Assink, J.W.; Hanemaaijer, J.H.; Van Medevoort, J.; Van Sonsbeek, E. Development and pilot testing of full-scale membrane distillation modules for deployment of waste heat. *Desalination* **2013**, *323*, 55–65. [CrossRef]
49. Zhani, K.; Zarzoum, K.; Ben Bacha, H.; Koschikowski, J.; Pfeifle, D. Autonomous solar powered membrane distillation systems: State of the art. *Desalination Water Treat.* **2016**, *57*, 23038–23051. [CrossRef]
50. Guillén-Burrieza, E.; Blanco, J.; Zaragoza, G.; Alarcón, D.C.; Palenzuela, P.; Ibarra, M.; Gernjak, W. Experimental analysis of an air gap membrane distillation solar desalination pilot system. *J. Membr. Sci.* **2011**, *379*, 386–396. [CrossRef]
51. Wang, P.; Chung, T.S. Recent advances in membrane distillation processes: Membrane development, configuration design and application exploring. *J. Membr. Sci.* **2015**, *474*, 39–56. [CrossRef]
52. Camacho, L.M.; Dumée, L.; Zhang, J.; Li, J.D.; Duke, M.; Gomez, J.; Gray, S. Advances in membrane distillation for water desalination and purification applications. *Water* **2013**, *5*, 94–196. [CrossRef]
53. Köhler, W.; Wiegand, S. (Eds.) . *Thermal Nonequilibrium Phenomena in Fluid Mixtures*; Springer: Cham, Switzerland, 2008; Volume 584.
54. Würger, A. Is Soret equilibrium a non-equilibrium effect? *C. R. Mécanique* **2013**, *341*, 438–448. [CrossRef]
55. Curcio, E.; Drioli, E. Membrane distillation and related operations—A review. *Sep. Purif. Rev.* **2005**, *34*, 35–86. [CrossRef]
56. Winter, D.; Koschikowski, J.; Wieghaus, M. Desalination Using Membrane Distillation: Experimental Studies on Full Scale Spiral Wound Modules. *J. Membr. Sci.* **2011**, *370*, 104–112. [CrossRef]

57. Ali, A.; Macedonio, F.; Drioli, E.; Aljlil, S.; Alharbi, O.A. Experimental and Theoretical Evaluation of Temperature Polarization Phenomenon in Direct Contact Membrane Distillation. *Chem. Eng. Res. Des.* **2013**, *91*, 1966–1977. [CrossRef]
58. Lawson, K.W.; Lloyd, D.R. Membrane Distillation. *J. Membr. Sci.* **1997**, *124*, 1–25. [CrossRef]
59. Bird, R.B.; Stewart, W.E.; Lightfoot, E.N. *Transport Phenomena*; Wiley: New York, NY, USA, 1960.
60. Mason, E.A.; Malinauskas, A.P. *Gas Transport in Porous Media: The Dusty-Gas Model*; Elsevier: New York, NY, USA, 1983.
61. Al-Anezi, A.A.H.; Sharif, A.O.; Sanduk, M.I.; Khan, A.R. Experimental investigation of heat and mass transfer in tubular membrane distillation module for desalination. *Int. Sch. Res. Notices* **2012**, *2012*, 738731. [CrossRef]
62. Eykens, L.; De Sitter, K.; Dotremont, C.; Pinoy, L.; Van der Bruggen, B. Membrane synthesis for membrane distillation: A review. *Sep. Purif. Technol.* **2017**, *182*, 36–51. [CrossRef]
63. Chew, N.G.P.; Zhao, S.; Loh, C.H.; Permogorov, N.; Wang, R. Surfactant effects on water recovery from produced water via direct-contact membrane distillation. *J. Membr. Sci.* **2017**, *528*, 126–134. [CrossRef]
64. Rezaei, M.; Warsinger, D.M.; Duke, M.C.; Matsuura, T.; Samhaber, W.M. Wetting phenomena in membrane distillation: Mechanisms, reversal, and prevention. *Water Res.* **2018**, *139*, 329–352. [CrossRef] [PubMed]
65. Feng, C.; Wang, R.; Shi, B.; Li, G.; Wu, Y. Factors affecting pore structure and performance of poly (vinylidene fluoride-co-hexafluoro propylene) asymmetric porous membrane. *J. Membr. Sci.* **2006**, *277*, 55–64. [CrossRef]
66. Cui, Z.; Drioli, E.; Lee, Y.M. Recent progress in fluoropolymers for membranes. *Prog. Polym. Sci.* **2014**, *39*, 164–198. [CrossRef]
67. Li, N.N.; Fane, A.G.; Ho, W.W.; Matsuura, T. (Eds.) . *Advanced Membrane Technology and Applications*; John Wiley & Sons: Hoboken, NJ, USA, 2011.
68. Drioli, E.; Giorno, L.; Fontananova, E. (Eds.) *Comprehensive Membrane Science and Engineering*; Elsevier: Amsterdam, The Netherlands, 2017.
69. Jung, J.T.; Kim, J.F.; Wang, H.H.; Di Nicolo, E.; Drioli, E.; Lee, Y.M. Understanding the non-solvent induced phase separation (NIPS) effect during the fabrication of microporous PVDF membranes via thermally induced phase separation (TIPS). *J. Membr. Sci.* **2016**, *514*, 250–263. [CrossRef]
70. Kim, J.F.; Jung, J.T.; Wang, H.H.; Lee, S.Y.; Moore, T.; Sanguineti, A.; Drioli, E.; Lee, Y.M. Microporous PVDF membranes via thermally induced phase separation (TIPS) and stretching methods. *J. Membr. Sci.* **2016**, *509*, 94–104. [CrossRef]
71. Liu, F.; Hashim, N.A.; Liu, Y.; Abed, M.R.M.; Li, K. Progress in the Production and Modification of PVDF Membranes. *J. Membr. Sci.* **2011**, *375*, 1–27. [CrossRef]
72. Tijing, L.D.; Choi, J.; Lee, S.; Kim, S.; Kyong, H. Recent Progress of Membrane Distillation Using Electrospun Nanofibrous Membrane. *J. Membr. Sci.* **2014**, *453*, 435–462. [CrossRef]
73. Gugliuzza, A.; Drioli, E. New performance of hydrophobic fluorinated porous membranes exhibiting particulate-like morphology. *Desalination* **2009**, *240*, 14. [CrossRef]
74. Mokhtar, N.M.; Lau, W.J.; Ismail, A.F.; Veerasamy, D. Membrane distillation technology for treatment of wastewater from rubber industry in Malaysia. *Procedia CIRP* **2015**, *26*, 792–796. [CrossRef]
75. Mokhtar, N.M.; Lau, W.J.; Ismail, A.F. Dye wastewater treatment by direct contact membrane distillation using polyvinylidene fluoride hollow fiber membranes. *J. Polym. Eng.* **2015**, *35*, 471–479. [CrossRef]
76. Feng, S.; Zhong, Z.; Wang, Y.; Xing, W.; Drioli, E. Progress and perspectives in PTFE membrane: Preparation, modification, and applications. *J. Membr. Sci.* **2018**, *549*, 332–349. [CrossRef]
77. Ragunath, S.; Roy, S.; Mitra, S. Carbon nanotube immobilized membrane with controlled nanotube incorporation via phase inversion polymerization for membrane distillation based desalination. *Sep. Purif. Technol.* **2018**, *194*, 249–255. [CrossRef]
78. Liu, G.; Pan, J.; Xu, X.; Wang, Z.; Cui, Z. Preparation of ECTFE porous membrane with a green diluent TOTM and performance in VMD process. *J. Membr. Sci.* **2020**, *612*, 118375. [CrossRef]
79. Gugliuzza, A.; Drioli, E. PVDF and HYFLON AD Membranes: Ideal Interfaces for Contactor Applications. *J. Membr. Sci.* **2007**, *300*, 51–62. [CrossRef]
80. Cui, Z.; Zhang, Y.; Li, X.; Wang, X.; Drioli, E.; Wang, Z.; Zhao, S. Optimization of novel composite membranes for water and mineral recovery by vacuum membrane distillation. *Desalination* **2018**, *440*, 39–47. [CrossRef]
81. He, Z.; Lyu, Z.; Gu, Q.; Zhang, L.; Wang, J. Ceramic-based membranes for water and wastewater treatment. *Colloids Surf. A Physicochem. Eng. Asp.* **2019**, *578*, 123513. [CrossRef]
82. Hubadillah, S.K.; Tai, Z.S.; Othman, M.H.D.; Harun, Z.; Jamalludin, M.R.; Rahman, M.A.; Jaafar, J.; Ismail, A.F. Hydrophobic ceramic membrane for membrane distillation: A mini review on preparation, characterization, and applications. *Sep. Purif. Technol.* **2019**, *217*, 71–84. [CrossRef]
83. Cerneaux, S.; Strużyńska, I.; Kujawski, W.M.; Persin, M.; Larbot, A. Comparison of various membrane distillation methods for desalination using hydrophobic ceramic membranes. *J. Membr. Sci.* **2009**, *337*, 55–60. [CrossRef]
84. Ramlow, H.; Ferreira, R.K.M.; Marangoni, C.; Machado, R.A.F. Ceramic membranes applied to membrane distillation: A comprehensive review. *Int. J. Appl. Ceram. Technol.* **2019**, *16*, 2161–2172. [CrossRef]
85. Larbot, A.; Gazagnes, L.; Krajewski, S.; Bukowska, M.; Kujawski, W. Water desalination using ceramic membrane distillation. *Desalination* **2004**, *168*, 367–372. [CrossRef]
86. Fang, H.; Gao, J.F.; Wang, H.T.; Chen, C.S. Hydrophobic porous alumina hollow fiber for water desalination via membrane distillation process. *J. Membr. Sci.* **2012**, *403*, 41–46. [CrossRef]

87. Ko, C.C.; Ali, A.; Drioli, E.; Tung, K.L.; Chen, C.H.; Chen, Y.R.; Macedonio, F. Performance of ceramic membrane in vacuum membrane distillation and in vacuum membrane crystallization. *Desalination* **2018**, *440*, 48–58. [CrossRef]
88. Maaskant, E.; de Wit, P.; Benes, N.E. Direct interfacial polymerization onto thin ceramic hollow fibers. *J. Membr. Sci.* **2018**, *550*, 296–301. [CrossRef]
89. Aroon, M.A.; Ismail, A.F.; Montazer-Rahmati, M.M.; Matsuura, T. Effect of raw multi-wall carbon nanotubes on morphology and separation properties of polyimide membranes. *Sep. Sci. Technol.* **2010**, *45*, 2287–2297. [CrossRef]
90. Chen, L.H.; Chen, Y.R.; Huang, A.; Chen, C.H.; Su, D.Y.; Hsu, C.C.; Tsai, F.Y.; Tung, K.L. Nanostructure depositions on alumina hollow fiber membranes for enhanced wetting resistance during membrane distillation. *J. Membr. Sci.* **2018**, *564*, 227–236. [CrossRef]
91. Sabir, A.; Islam, A.; Shafiq, M.; Shafeeq, A.; Butt, M.T.Z.; Ahmad, N.M.; Sanaullah, K.; Jamil, T. Novel polymer matrix composite membrane doped with fumed silica particles for reverse osmosis desalination. *Desalination* **2015**, *368*, 159–170. [CrossRef]
92. Camacho, L.M.; Pinion, T.A.; Olatunji, S.O. Behavior of mixed-matrix graphene oxide–polysulfone membranes in the process of direct contact membrane distillation. *Sep. Purif. Technol.* **2020**, *240*, 116645. [CrossRef]
93. Leaper, S.; Abdel-Karim, A.; Faki, B.; Luque-Alled, J.M.; Alberto, M.; Vijayaraghavan, A.; Holmes, S.M.; Szekely, G.; Badawy, M.I.; Shokri, N.; et al. Flux-enhanced PVDF mixed matrix membranes incorporating APTS-functionalized graphene oxide for membrane distillation. *J. Membr. Sci.* **2018**, *554*, 309–323. [CrossRef]
94. Bonyadi, S.; Chung, T.S. Flux enhancement in membrane distillation by fabrication of dual layer hydrophilic–hydrophobic hollow fiber membranes. *J. Membr. Sci.* **2007**, *306*, 134–146. [CrossRef]
95. Dastbaz, A.; Karimi-Sabet, J.; Ahadi, H.; Amini, Y. Preparation and characterization of novel modified PVDF-HFP/GO/ODS composite hollow fiber membrane for Caspian Sea water desalination. *Desalination* **2017**, *424*, 62–73. [CrossRef]
96. Gontarek, E.; Macedonio, F.; Militano, F.; Giorno, L.; Lieder, M.; Politano, A.; Drioli, E.; Gugliuzza, A. Adsorption-assisted transport of water vapour in super-hydrophobic membranes filled with multilayer graphene platelets. *Nanoscale* **2019**, *11*, 11521–11529. [CrossRef]
97. Frappa, M.; Castillo, A.D.R.; Macedonio, F.; Politano, A.; Drioli, E.; Bonaccorso, F.; Pellegrini, V.; Gugliuzza, A. A few-layer graphene for advanced composite PVDF membranes dedicated to water desalination: A comparative study. *Nanoscale Adv.* **2020**, *2*, 4728–4739. [CrossRef]
98. Politano, A.; Bonaccorso, F.; Del Rio Castillo, A.E.; Drioli, E.; Gugliuzza, A.; Macedonio, F.; Pellegrini, V. A Procedure to Fabricate a Nanocomposite Membrane with Bidimensional Crystals Obtained through Exfoliation of Layered Materials by Wet-Jet Milling Technique. Italian Patent IT102018000020641, 22 November 2020.
99. Li, Y.X.; Cao, Y.; Wang, M.; Xu, Z.L.; Zhang, H.Z.; Liu, X.W.; Li, Z. Novel high-flux polyamide/TiO_2 composite nanofiltration membranes on ceramic hollow fibre substrates. *J. Membr. Sci.* **2018**, *565*, 322–330. [CrossRef]
100. Prince, J.A.; Singh, G.; Rana, D.; Matsuura, T.; Anbharasi, V.; Shanmugasundaram, T.S. Preparation and characterization of highly hydrophobic poly (vinylidene fluoride)–Clay nanocomposite nanofiber membranes (PVDF–clay NNMs) for desalination using direct contact membrane distillation. *J. Membr. Sci.* **2012**, *397*, 80–86. [CrossRef]
101. Hou, D.; Dai, G.; Wang, J.; Fan, H.; Zhang, L.; Luan, Z. Preparation and characterization of PVDF/nonwoven fabric flat-sheet composite membranes for desalination through direct contact membrane distillation. *Sep. Purif. Technol.* **2012**, *101*, 1–10. [CrossRef]
102. Zhang, J.; Song, Z.; Li, B.; Wang, Q.; Wang, S. Fabrication and characterization of superhydrophobic poly (vinylidene fluoride) membrane for direct contact membrane distillation. *Desalination* **2013**, *324*, 1–9. [CrossRef]
103. Meng, B.; Liu, G.; Mao, Y.; Liang, F.; Liu, G.; Jin, W. Fabrication of surface-charged MXene membrane and its application for water desalination. *J. Membr. Sci.* **2021**, *623*, 119076. [CrossRef]
104. Garofalo, A.; Carnevale, M.C.; Donato, L.; Drioli, E.; Alharbi, O.; Aljlil, S.A.; Criscuoli, A.; Algieri, C. Scale-up of MFI zeolite membranes for desalination by vacuum membrane distillation. *Desalination* **2016**, *397*, 205–212. [CrossRef]
105. Wu, X.Q.; Mirza, N.R.; Huang, Z.; Zhang, J.; Zheng, Y.M.; Xiang, J.; Xie, Z. Enhanced desalination performance of aluminium fumarate MOF-incorporated electrospun nanofiber membrane with bead-on-string structure for membrane distillation. *Desalination* **2021**, *520*, 115338. [CrossRef]
106. Frappa, M.; Castillo, A.D.R.; Macedonio, F.; Di Luca, G.; Drioli, E.; Gugliuzza, A. Exfoliated Bi_2Te_3-enabled membranes for new concept water desalination: Freshwater production meets new routes. *Water Res.* **2021**, *203*, 117503. [CrossRef] [PubMed]
107. Bhadra, M.; Roy, S.; Mitra, S. Flux enhancement in direct contact membrane distillation by implementing carbon nanotube immobilized PTFE membrane. *Sep. Purif. Technol.* **2016**, *161*, 136–143. [CrossRef]
108. Roy, S.; Bhadra, M.; Mitra, S. Enhanced desalination via functionalized carbon nanotube immobilized membrane in direct contact membrane distillation. *Sep. Purif. Technol.* **2014**, *136*, 58–65. [CrossRef]
109. Silva, T.L.; Morales-Torres, S.; Figueiredo, J.L.; Silva, A.M. Multi-walled carbon nanotube/PVDF blended membranes with sponge-and finger-like pores for direct contact membrane distillation. *Desalination* **2015**, *357*, 233–245. [CrossRef]
110. Dumée, L.F.; Sears, K.; Schütz, J.; Finn, N.; Huynh, C.; Hawkins, S.; Duke, M.; Gray, S. Characterization and evaluation of carbon nanotube Bucky-Paper membranes for direct contact membrane distillation. *J. Membr. Sci.* **2010**, *351*, 36–43. [CrossRef]
111. Barrejón, M.; Prato, M. Carbon nanotube membranes in water treatment applications. *Adv. Mater. Interfaces* **2022**, *9*, 2101260. [CrossRef]
112. Cheng, D.Y.; Wiersma, S.J. Composite membrane for a membrane distillation system. U.S. Patent 4,419,242, 6 December 1983.

113. Zuo, J.; Chung, T.S.; O'Brien, G.S.; Kosar, W. Hydrophobic/hydrophilic PVDF/Ultem® dual-layer hollow fiber membranes with enhanced mechanical properties for vacuum membrane distillation. *J. Membr. Sci.* **2017**, *523*, 103–110. [CrossRef]
114. Zou, L.; Zhang, X.; Gusnawan, P.; Zhang, G.; Yu, J. Crosslinked PVDF based hydrophilic-hydrophobic dual-layer hollow fiber membranes for direct contact membrane distillation desalination: From the seawater to oilfield produced water. *J. Membr. Sci.* **2021**, *619*, 118802. [CrossRef]
115. Santoro, S.; Avci, A.H.; Politano, A.; Curcio, E. The advent of thermoplasmonic membrane distillation. *Chem. Soc. Rev.* **2022**, *51*, 6087–6125. [CrossRef] [PubMed]
116. Koschikowski, J.; Wieghaus, M.; Rommel, M. Solar thermal-driven desalination plants based on membrane distillation. *Desalination* **2003**, *156*, 295–304. [CrossRef]
117. Wang, X.; Zhang, L.; Yang, H.; Chen, H. Feasibility research of potable water production via solar-heated hollow fiber membrane distillation system. *Desalination* **2009**, *247*, 403–411. [CrossRef]
118. Saffarini, R.B.; Summers, E.K.; Arafat, H.A. Technical evaluation of stand-alone solar powered membrane distillation systems. *Desalination* **2012**, *286*, 332–341. [CrossRef]
119. Hejazi, M.A.A.; Bamaga, O.A.; Al-Beirutty, M.H.; Gzara, L.; Abulkhair, H. Effect of intermittent operation on performance of a solar-powered membrane distillation system. *Sep. Purif. Technol.* **2019**, *220*, 300–308. [CrossRef]
120. Zhang, P.; Liao, Q.; Yao, H.; Huang, Y.; Cheng, H.; Qu, L. Direct solar steam generation system for clean water production. *Energy Storage Mat.* **2019**, *18*, 429–446. [CrossRef]
121. Shi, L.; Wang, X.; Hu, Y.; He, Y.; Yan, Y. Solar-thermal conversion and steam generation: A review. *Appl. Therm. Eng.* **2020**, *179*, 115691. [CrossRef]
122. Huang, Q.; Liang, X.; Yan, C.; Liu, Y. Review of interface solar-driven steam generation systems: High-efficiency strategies, applications and challenges. *Appl. Energy* **2021**, *283*, 116361. [CrossRef]
123. Cazalilla, M.A.; Dolado, J.S.; Rubio, A.; Echenique, P.M. Plasmonic excitations in noble metals: The case of Ag. *Phys. Rev. B* **2000**, *61*, 8033. [CrossRef]
124. Politano, A. Interplay of structural and temperature effects on plasmonic excitations at noble-metal interfaces. *Philos. Mag.* **2012**, *92*, 768–778. [CrossRef]
125. Politano, A.; Chiarello, G. The influence of electron confinement, quantum size effects, and film morphology on the dispersion and the damping of plasmonic modes in Ag and Au thin films. *Prog. Surf. Sci.* **2015**, *90*, 144–193.
126. Rodríguez-Oliveros, R.; Sánchez-Gil, J.A. Gold nanostars as thermoplasmonic nanoparticles for optical heating. *Opt. Express* **2012**, *20*, 621–626. [CrossRef] [PubMed]
127. Lyvers, D.P.; Moon, J.M.; Kildishev, A.V.; Shalaev, V.M.; Wei, A. Gold nanorod arrays as plasmonic cavity resonators. *ACS Nano* **2008**, *2*, 2569–2576. [CrossRef]
128. Politano, A.; Formoso, V.; Chiarello, G. Dispersion and damping of gold surface plasmon. *Plasmonics* **2008**, *3*, 165–170. [CrossRef]
129. Politano, A.; Argurio, P.; Di Profio, G.; Sanna, V.; Cupolillo, A.; Chakraborty, S.; Arafat, H.A.; Curcio, E. Photothermal membrane distillation for seawater desalination. *Adv. Mater.* **2017**, *29*, 1603504. [CrossRef]
130. Susman, M.D.; Feldman, Y.; Vaskevich, A.; Rubinstein, I. Chemical deposition and stabilization of plasmonic copper nanoparticle films on transparent substrates. *Chem. Mater.* **2012**, *24*, 2501–2508. [CrossRef]
131. Chong, X.; Abboud, J.; Zhang, Z. Plasmonics resonance enhanced active photothermal effects of aluminum and iron nanoparticles. *J. Nanosci. Nanotechnol.* **2015**, *15*, 2234–2240. [CrossRef]
132. Amendola, V.; Saija, R.; Maragò, O.M.; Iatì, M.A. Superior plasmon absorption in iron-doped gold nanoparticles. *Nanoscale* **2015**, *7*, 8782–8792. [CrossRef]
133. Kravets, V.G.; Jalil, R.; Kim, Y.J.; Ansell, D.; Aznakayeva, D.E.; Thackray, B.; Britnell, L.; Belle, B.D.; Withers, F.; Radko, I.P.; et al. Graphene-protected copper and silver plasmonics. *Scientific reports* **2014**, *4*, 1–8.
134. Sarina, S.; Zhu, H.; Jaatinen, E.; Xiao, Q.; Liu, H.; Jia, J.; Chen, C.; Zhao, J. Enhancing catalytic performance of palladium in gold and palladium alloy nanoparticles for organic synthesis reactions through visible light irradiation at ambient temperatures. *J. Am. Chem. Soc.* **2013**, *135*, 5793–5801. [CrossRef] [PubMed]
135. Lin, T.; Yang, C.; Wang, Z.; Yin, H.; Lü, X.; Huang, F.; Lin, J.; Xie, X.; Jiang, M. Effective nonmetal incorporation in black titania with enhanced solar energy utilization. *Energy Environ. Sci.* **2014**, *7*, 967–972. [CrossRef]
136. Farid, M.U.; Kharraz, J.A.; An, A.K. Plasmonic titanium nitride nano-enabled membranes with high structural stability for efficient photothermal desalination. *ACS Appl. Mater. Interfaces* **2021**, *13*, 3805–3815. [CrossRef] [PubMed]
137. Wu, X.; Robson, M.E.; Phelps, J.L.; Tan, J.S.; Shao, B.; Owens, G.; Xu, H. A flexible photothermal cotton-CuS nanocage-agarose aerogel towards portable solar steam generation. *Nano Energy* **2019**, *56*, 708–715. [CrossRef]
138. Yang, X.; Yang, Y.; Fu, L.; Zou, M.; Li, Z.; Cao, A.; Yuan, Q. An ultrathin flexible 2D membrane based on single-walled nanotube–MoS_2 hybrid film for high-performance solar steam generation. *Adv. Funct. Mater.* **2018**, *28*, 1704505. [CrossRef]
139. Ghim, D.; Wu, X.; Suazo, M.; Jun, Y.S. Achieving maximum recovery of latent heat in photothermally driven multi-layer stacked membrane distillation. *Nano Energy* **2021**, *80*, 105444. [CrossRef]
140. Wang, Y.; Wang, C.; Song, X.; Megarajan, S.K.; Jiang, H. A facile nanocomposite strategy to fabricate a rGO–MWCNT photothermal layer for efficient water evaporation. *J. Mater. Chem. A* **2018**, *6*, 963–971. [CrossRef]
141. Wang, X.; He, Y.; Liu, X.; Zhu, J. Enhanced direct steam generation via a bio-inspired solar heating method using carbon nanotube films. *Powder Technol.* **2017**, *321*, 276–285. [CrossRef]

142. Dongare, P.D.; Alabastri, A.; Pedersen, S.; Zodrow, K.R.; Hogan, N.J.; Neumann, O.; Wu, J.; Wang, T.; Deshmukh, A.; Elimelech, M.; et al. Nanophotonics-enabled solar membrane distillation for off-grid water purification. *Proc. Natl. Acad. Sci. USA* **2017**, *114*, 6936–6941. [CrossRef]
143. Han, X.; Wang, W.; Zuo, K.; Chen, L.; Yuan, L.; Liang, J.; Li, Q.; Ajayan, P.M.; Zhao, Y.; Lou, J. Bio-derived ultrathin membrane for solar driven water purification. *Nano Energy* **2019**, *60*, 567–575. [CrossRef]
144. Jiang, B.P.; Zhang, L.; Zhu, Y.; Shen, X.C.; Ji, S.C.; Tan, X.Y.; Cheng, L.; Liang, H. Water-soluble hyaluronic acid–hybridized polyaniline nanoparticles for effectively targeted photothermal therapy. *J. Mater. Chem. B* **2015**, *3*, 3767–3776. [CrossRef] [PubMed]
145. Zou, Q.; Huang, J.; Zhang, X. One-step synthesis of iodinated polypyrrole nanoparticles for CT imaging guided photothermal therapy of tumors. *Small* **2018**, *14*, 1803101. [CrossRef] [PubMed]
146. Peng, Y.; Wang, Y.; Li, W.; Jin, J. Bio-inspired vertically aligned polyaniline nanofiber layers enabling extremely high-efficiency solar membrane distillation for water purification. *J. Mater. Chem. A* **2021**, *9*, 10678–10684. [CrossRef]